

## SPECIAL ARTICLE

# SARS-CoV-2: what it is, how it acts, and how it manifests in imaging studies<sup>☆</sup>



G.C. Fernández-Pérez<sup>a,\*</sup>, M. Oñate Miranda<sup>a</sup>, P. Fernández-Rodríguez<sup>b</sup>,  
M. Velasco Casares<sup>a</sup>, M. Corral de la Calle<sup>c</sup>, Á. Franco López<sup>d</sup>, M. Díez Blanco<sup>a</sup>,  
J.M. Oñate Cuchat<sup>e</sup>

<sup>a</sup> Servicio de Radiodiagnóstico, Hospital Universitario Río Hortega, Valladolid, Spain

<sup>b</sup> Servicio de Medicina Nuclear, Hospital Virgen del Rocío, Sevilla, Spain

<sup>c</sup> Servicio de Radiodiagnóstico, Hospital Nuestra Señora de Sonsoles, Ávila, Spain

<sup>d</sup> Servicio Radiodiagnóstico, Hospital Universitario Vinalopó, Alicante, Spain

<sup>e</sup> Servicio de Anatomía Patológica, Hospital Universitario Río Hortega, Valladolid, Spain

Received 9 May 2020; accepted 14 October 2020

Available online 5 February 2021

## KEYWORDS

SARS-CoV-2;  
SARS-2;  
COVID-19;  
High-resolution CT;  
Dual-energy CT;  
Lung perfusion blood  
volume;  
PET/TC

**Abstract** COVID-19 is a disease with many clinical, biochemical, and radiological signs that has a predilection for the lungs, probably because of the high number of ACE-2 receptors in this organ. The infection of cells activates proinflammatory substances, causing diffuse alveolar damage, which is the histopathological basis of ARDS. The exudative phase would manifest as ground-glass opacities and consolidation, and the proliferative phase would manifest as a tendency toward a more linear morphology. Both CT and PET/CT findings support the inflammatory character of the lung lesions in the initial phase of the disease and in patients with mild-moderate disease.

Severe cases have pulmonary hypoperfusion that is likely due to abnormal alveolar ventilation and perfusion. On the other hand, a prothrombotic state increases the risk of thromboembolic disease through the activation of coagulation and platelet pathways with the production of fibrin degradation products (D-dimer) and consumption of platelets.

© 2020 SERAM. Published by Elsevier España, S.L.U. All rights reserved.

<sup>☆</sup> Please cite this article as: Fernández-Pérez GC, Oñate Miranda M, Fernández-Rodríguez P, Velasco Casares M, Corral de la Calle M, Franco López Á, et al. SARS-CoV-2: cómo es, cómo actúa y cómo se expresa en la imagen. Radiología. 2021;63:115–126.

\* Corresponding author.

E-mail address: gabriel.fdez.perez@gmail.com (G.C. Fernández-Pérez).

**PALABRAS CLAVE**

SARS-CoV-2;  
 SARS-2;  
 COVID-19;  
 TC alta resolución;  
 TC doble energía;  
 Percusión pulmonar  
 PBV;  
 PET/TC

**SARS-CoV-2: cómo es, cómo actúa y cómo se expresa en la imagen**

**Resumen** La COVID-19 es una enfermedad con una gran semiología clínica, bioquímica y radiológica, que tiene una afectación preferente por el pulmón, probablemente debido a un mayor número de receptores ECA-2. La infección celular activa sustancias proinflamatorias y provoca un daño alveolar difuso, que es la base histopatológica del distrés respiratorio del adulto. La fase exudativa explicaría las imágenes “en vidrio deslustrado” y consolidación, mientras que la tendencia hacia una morfología más lineal representa la fase proliferativa. Tanto la tomografía computarizada (TC) como la tomografía por emisión de positrones/ tomografía computarizada (PET/TC) apoyan el carácter inflamatorio de las lesiones pulmonares cuando la enfermedad está en fase inicial o es leve-moderada.

Los casos graves muestran una hipoperfusión pulmonar que se explicaría por una alteración de la ventilación-perfusión alveolar (V/Q). Por otro lado, un estado protrombótico conlleva mayor probabilidad de enfermedad tromboembólica por la activación de la vía de la coagulación y plaquetaria, con la producción de sustancia de degradación de la fibrina (dímero D) así como el consumo de plaquetas.

© 2020 SERAM. Publicado por Elsevier España, S.L.U. Todos los derechos reservados.

**History**

COVID-19, the disease caused by the SARS-CoV-2 coronavirus, is currently a global pandemic. This pandemic is one of the most active over the centuries, with close to 1.4 million deaths around the world (at the time of drafting of this paper). Spain is one of the countries with the highest number of deaths per million inhabitants.

On 31 December 2019, the Wuhan Health Commission notified the Chinese Center for Disease Control and Prevention and the World Health Organization (WHO) of a group of 27 patients with pneumonia of unknown origin. Contact tracing of those patients revealed a link to the Huanan Seafood Wholesale Market in Wuhan, which sells living and dead animals of multiple species, including bats, snakes and pangolins. The outbreak of infection was thought to stem from a virus mutation that enabled transmission from animals to humans. On 30 January 2020, the WHO declared the viral pneumonia outbreak a public health emergency of international concern. On 11 March 2020, it characterised it as a pandemic of coronavirus disease 2019 (COVID-19).<sup>1,2</sup>

**Virology**

On 7 January 2020, the origin of the infection was discovered in China; on 11 February, the WHO named it 2019 novel [new] coronavirus (2019-nCoV). The disease was sometimes colloquially called Wuhan pneumonia; but the WHO renamed it COVID-19 to avoid stigmatising a particular geographic area. On very nearly the same day, the International Committee on Taxonomy of Viruses named the causative virus severe acute respiratory syndrome coronavirus 2 (SARS-CoV-2), or SARS-2 to distinguish it from the SARS-1 outbreak of 2002–2003.<sup>3,4</sup>

Coronaviruses belong to the family *Coronaviridae* and are a type of enveloped single-stranded RNA virus. They are divided into four genera: alpha, beta, gamma and delta. To date, seven coronaviruses have been identified in humans,

all of which are members of the alpha and beta genera. The beta genus includes the SARS-1, SARS-2 and Middle East respiratory syndrome (MERS) coronaviruses. Coronaviruses belonging to the alpha genus normally cause signs and symptoms of the common cold. Those belonging to the beta genus sometimes cause acute respiratory distress syndrome (ARDS) in adults.<sup>5,6</sup> These viruses arise from virus mutations in animals such as bats, which act as reservoirs before contaminating or spreading to hosts (humans). SARS-2 has been linked to the genome of a virus found in horseshoe bats, which belong to the species *Rhinolophus*, in the Chinese province of Yunnan (96% similarity). Early on, it was postulated that pangolins serve as intermediate hosts or even primary reservoirs (Pangolin-Cov), but this has not been confirmed.<sup>3,7</sup>

SARS-CoV-2 (hereinafter, SARS-2) has a diameter of 50–200 nm (Fig. 1A). Among its surface proteins, the spike (S) glycoprotein is the one that binds to the host cell through angiotensin-converting enzyme 2 (ACE2) receptors.<sup>3</sup> These receptors, present in type II lung cells, are also found in smaller numbers in the kidneys, bowel, heart, uterus, brain, vascular walls and adrenal glands (Fig. 1B).<sup>8–10</sup> Once the virus binds to the cell membrane through a mechanism of endocytosis, the RNA virus genome is released into the cytoplasm for replication. The genomic RNA, using the cell's endoplasmic reticulum and Golgi bodies, prepares nucleocapsids to form intracellular virions and new viral particles that exit the cell through exocytosis. The cell, having been altered functionally and structurally, undergoes apoptosis (programmed cell death)<sup>11,12</sup> (Fig. 1C).

Cytokines are released, very likely as a result of interaction between the M protein of the virus inside the cell and the nuclear cytosol. These cytokines then activate cells such as monocytes, T lymphocytes, macrophages, endothelial cells, epithelial cells and dendritic cells. This mechanism of innate immunity in the host represents the first line of defence against the virus. Subsequently, through activation

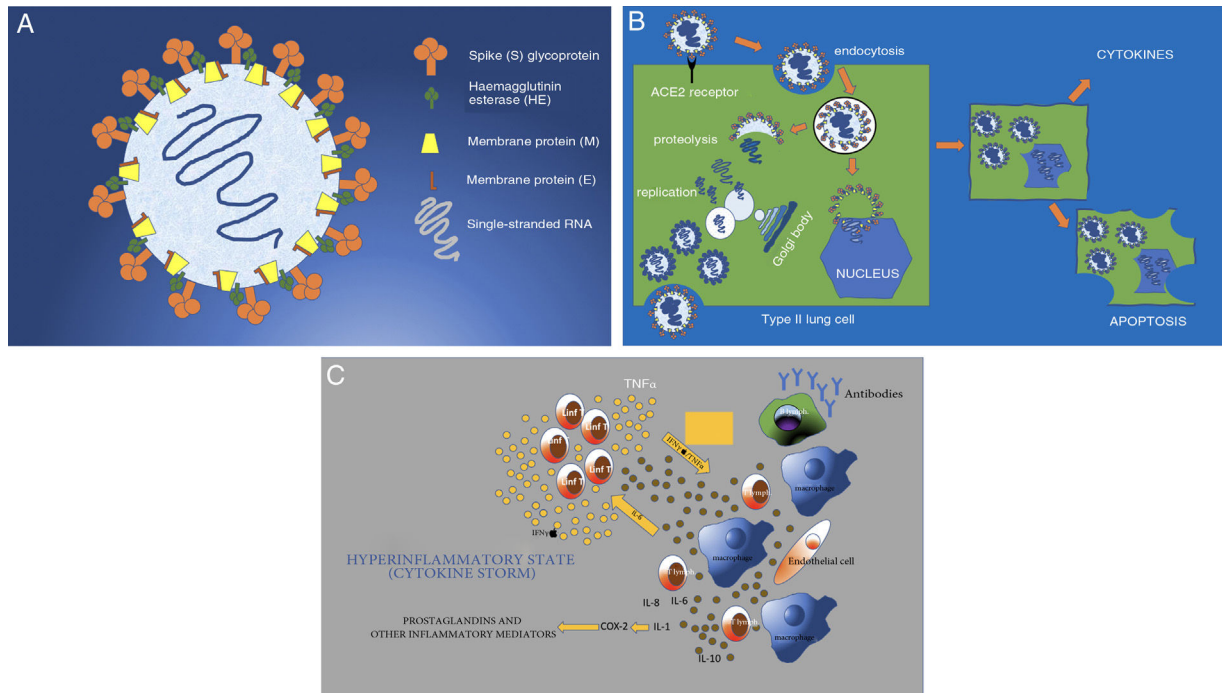


**Figure 1** A) Structure of SARS-CoV-2 (SARS-2). Enveloped single-stranded RNA virus with surface glycoproteins. The virus's S or spike protein gives it its characteristic crown-like shape and binds to ACE2 receptors on cells. B) SARS-2 virus infection and replication. The virus binds to the ACE2 receptors of the host cell (in this case, the type II lung cell) to enter the cell by endocytosis through the cell membrane. The viral envelope is destroyed through proteolysis; this releases the RNA, which replicates and then, through the membranes of the cell's Golgi bodies and endoplasmic reticulum, forms complete virions (viral inclusions in tissues on autopsy). These virions are eliminated by means of exocytosis through the cell membrane. Other virus proteins enable the virus to enter the nucleus and alter it structurally and functionally, leading to apoptosis, or programmed cell death. C) The cell involvement caused by the virus prompts activation of macrophages, endothelial cells, dendritic cells, etc. These produce cytokines (IL-1, IL-6 and IL-8) and cause T lymphocytes to activate as a rapid immune response. However, a response that is not rapid (delayed response) or simply not well regulated causes overproduction through IFN and TNF, resulting in greater activation of macrophages and other cells (cytokine storm). COX-2: cyclooxygenase-2; IFN: interferon; IL: interleukin; TNF: tumour necrosis factor.

of B lymphocytes, antibodies are generated to destroy the virus and clear it from the body.

Observation of patients with SARS and MERS coronaviruses has suggested that the immune mechanism may be poorly regulated, such that macrophages and T lymphocytes overproduce or hyper-regulate cytokines, resulting in systemic inflammatory response syndrome (SIRS), also called cytokine storm. A rapid, well-coordinated innate immune response against viral infection would keep the virus from replicating and prevent its effects, but a poorly regulated or excessive immune response could cause cell damage.<sup>13</sup> Experiments with cells *in vitro* have demonstrated delayed release of cytokines and other kinins in respiratory epithelial cells, dendritic cells and macrophages early in the course of SARS-2 infection. Cells later secrete interferon (IFN) antiviral factors and high levels of pro-inflammatory cytokines such as interleukins (ILs) (IL-1 and IL-6) and tumour necrosis factor (TNF). Secretion of these substances induces further production and release of cytokines, which cause severe cell damage.<sup>14,15</sup>

SARS-2, like SARS-1 and MERS, infects epithelial cells in human airways (type II lung cells), where THP-1 cells (members of a monocytic cell line), macrophages and dendritic cells induce delayed but elevated levels of pro-inflammatory substances. Serum cytokine and chemokine levels are signifi-

cantly higher in patients with severe disease than in patients with milder disease.

From these studies, it may be gleaned that a poorly controlled, exaggerated cytokine response by cells infected with SARS-2 could play a significant role in COVID-19's pathogenesis and progression towards severe stages of ARDS.<sup>16</sup>

## Signs and symptoms

Signs and symptoms can be categorised into five groups:

- 1 No signs or symptoms (asymptomatic).
- 2 Mild to moderate disease (80%).
- 3 Severe disease and hospitalisation (13%).
- 4 Critical disease and intensive care unit (ICU) admission (5%).
- 5 Death (2%).

The true percentage of asymptomatic patients is difficult to ascertain. Zhu et al. published a meta-analysis of 38 studies that enrolled a population of 3062 patients with COVID-19, 12% of whom were asymptomatic.<sup>17</sup> On the Diamond Princess cruise ship, out of 634 patients with a positive reverse transcription-polymerase chain reaction (RT-PCR) test, the actual proportion of asymptomatic patients was

18%.<sup>17,18</sup> Men and women are affected similarly, with slightly higher rates in men (50%–62%).<sup>18</sup>

The most common symptom is fever (80%–98%), in the evening; in many cases, it is high and accompanied by chills and sweating. Cough is the second most common symptom (63%–70%). Usually it is dry, though in 30%–40% of patients it is accompanied by expectoration. There is a highly characteristic association with muscle pain (45%), severe weakness (asthenia) and tiredness. Anorexia has been observed in 39% of patients and usually accounts for weight loss, along with loss of taste and smell.<sup>19–21</sup> Signs in children tend to be milder and may even go unnoticed, though links to vasculitis, Kawasaki disease and multisystem inflammatory syndrome in children have been found.<sup>22</sup> Children are also more prone to skin problems such as rashes, urticarial lesions and pernio-like acral ischaemia.<sup>23,24</sup>

Dyspnoea is the most significant warning symptom (34%–50%); a combination of dyspnoea and O<sub>2</sub> desaturation indicates a serious clinical picture calling for hospital admission.

In terms of laboratory findings, lymphopenia is characteristic (57%), as are high acute-phase reactant levels (C-reactive protein [CRP] is elevated in 74% of patients, and erythrocyte sedimentation rate [ESR] is elevated in 66%) and high ferritin levels. Partial pressure of oxygen (PO<sub>2</sub>) is decreased in more than half of patients (64%), and it is not uncommon to find moderate alteration of liver enzymes (29%) without elevation of bilirubin.

One of the most striking abnormalities is elevation of D-dimer levels, associated in many cases with thrombocytopenia. These abnormalities have given rise to a hypothesis of disseminated intravascular coagulation (DIC). DIC, a disease that results from activation and stimulation of the

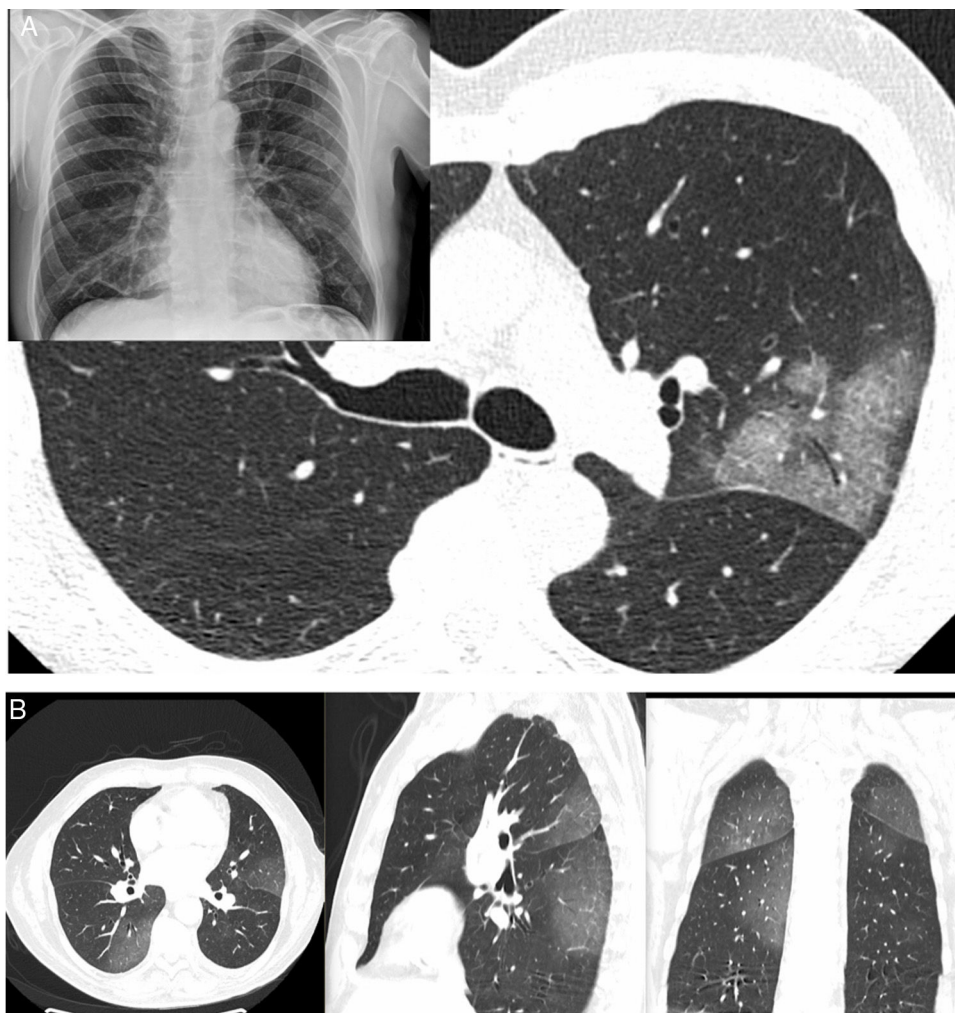


**Figure 2** A) A 61-year-old man (healthcare worker). He had fever, asthenia, muscle pain and cough for 4 days (positive PCR). In addition, a chest X-ray with blurring of the right cardiac silhouette (the patient had *pectus excavatum*) showed a subtle increase in density in the left upper lobe (LUL); as a result, a CT scan was ordered. The CT scan revealed a lesion with a crazy-paving pattern and air bronchogram in the LUL; no other lesions were seen anywhere else in the lung. B) A 66-year-old man had signs and symptoms suggestive of COVID-19 for 6 days. He had significant fever and cough with no notable expectoration. Ageusia and anosmia. No dyspnoea. Negative PCR. A CT scan showed increases in peripheral bilateral density with a posterior predominance, exhibiting a ground-glass pattern.

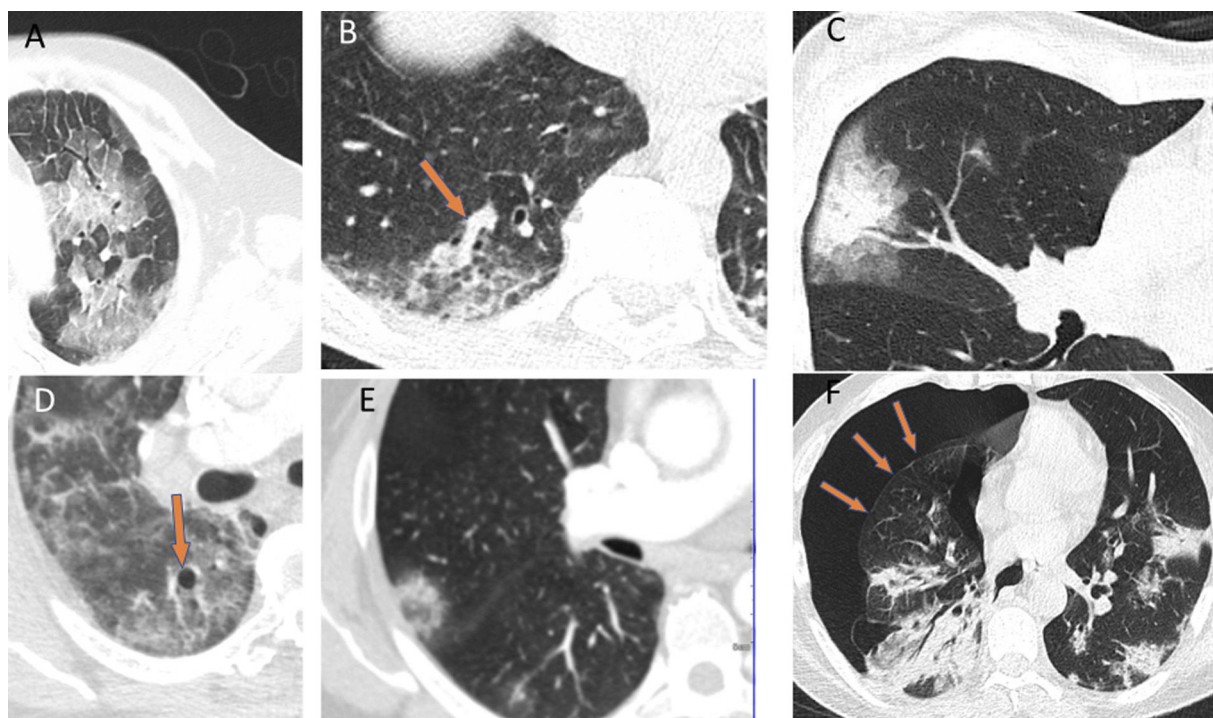


**Figure 3** Other radiological patterns on CT in patients with COVID-19: A) Crazy-paving pattern. B) Vascular thickening inside lesions. C) Halo sign. D) Vacuolisation. E) Reversed halo sign. F) Spontaneous pneumothorax.

coagulation system, causes thrombotic microangiopathy due to fibrin deposition and secondary fibrinolysis. It is common in many disease states, including infection and sepsis. However, clinical signs of DIC include bleeding, which is not usually seen in patients with COVID-19.<sup>25,26</sup>

### Radiological diagnosis

Chest X-rays have been very helpful in supporting patient triage and, in particular, serving as a criterion for deciding on hospital admission where patients have shown extensive radiological signs. Computed tomography (CT) is a test with high diagnostic reliability (98% sensitivity) that enables criteria for disease severity and progression to be evaluated. High-resolution studies show multifocal attenuation increases exhibiting ground-glass radiological patterns and consolidation with a bilateral peripheral distribution, with a slight predilection for the lower and posterior lung fields. This distribution was reported even in the first articles published on the subject. Single lesions are less commonly found (25%) and tend to be seen in the earliest stages of the disease (Fig. 2).<sup>27</sup>

The ground-glass pattern was the most common of the different radiological patterns (77%). Lymphadenopathy and pleural and pericardial effusion are atypical findings, except in severely ill and ICU-admitted patients, who may have secondary infections or heart failure. Other possible findings are: a crazy-paving pattern, the halo sign, the reversed halo sign, vascular thickening, air bronchogram, air cysts and, in some cases, spontaneous pneumothorax. However, the latter findings are less common and specific to this disease (Fig. 3).<sup>28–30</sup>

Authors such as Duan et al. and Berheim et al. documented the course of these patterns in relation to onset of symptoms, and divided COVID-19 into three stages: an early stage (0–2 days), an intermediate stage (3–5 days) and a late stage (6–12 days).<sup>31,32</sup> In the first few days (mean  $4 \pm 2$  days), it was not uncommon to find normal scans, or scans with a ground-glass pattern, either isolated (Fig. 2A) or multifocal (Fig. 2B). However, depending on the course of the disease, there could be overlapping or associated crazy-paving patterns and areas of consolidation that, in severe cases, converged to yield a radiological pattern of ARDS. Where the patient followed a favourable clinical course, these increases in density gradually decreased over the next two weeks, leaving reticular or linear images (fibrous stripes and subpleural lines). As of the third week, radiological imaging showed significant improvement with scant residual lesions. In some patients with mild to moderate disease who received treatment with corticosteroids, radiological clearance of lesions could be seen within a few days of treatment (Fig. 4).<sup>33</sup>

These radiological changes reflect the histological substrate reported in the autopsies and biopsies of patients with SARS-1 and COVID-19. The common histological finding is diffuse alveolar damage particular to ARDS in its different stages.<sup>34–36</sup> The first few days correspond to an early or exudative stage, characterised by diffuse alveolar damage with acute interstitial oedema, capillary congestion and exudate in the air space made up of fluid, fibrin and erythrocytes. These changes account for the radiological appearance of ground-glass and crazy-paving patterns. Vascular congestion could represent the *vascular thickening* sign seen on CT, which is reportedly characteristic of patients with COVID-19 (59% of patients with COVID-19 ver-

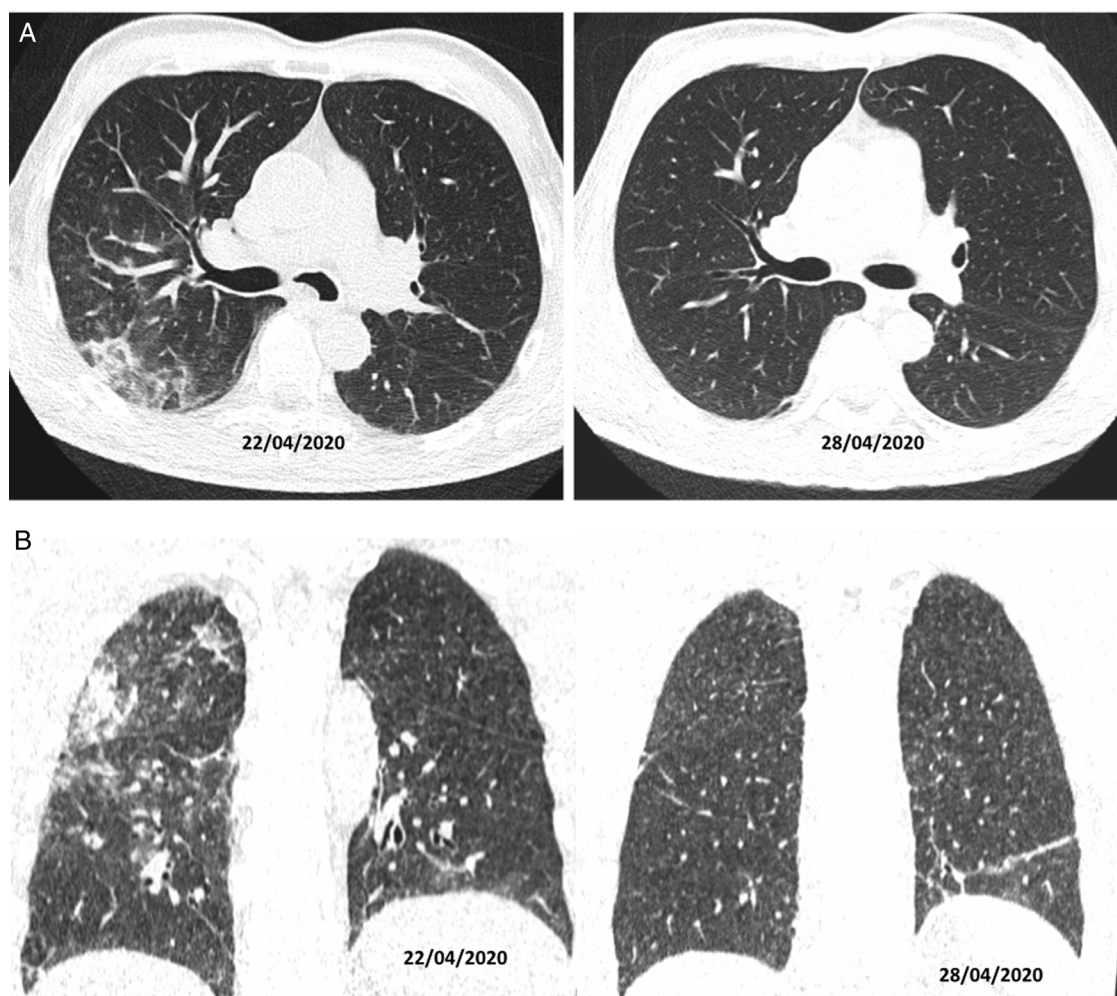


**Figure 4** CT on axial (A) and coronal (B) planes. A 56-year-old man, diabetic, with signs and symptoms of malaise and 39°C fever, without cough, for 10 days. He was treated with hydroxychloroquine, ceftriaxone and azithromycin. On his sixth day of admission, as he was not following a favourable clinical course, a decision was made to treat him with corticosteroids (22/04/2020); after four days of this treatment, he showed clinical and radiological improvement (28/04/2020).

sus 22% of patients with other forms of viral pneumonia).<sup>37</sup> In a later stage (after the first week), this exudate becomes more compact and takes on an eosinophilic appearance, with greater formation of hyaline membranes, especially along the walls of the alveolar ducts and distal respiratory bronchioles.<sup>38,39</sup> Radiologically, this is expressed as progression towards consolidation. The proliferative stage (from the second to the fourth week) shows changes with proliferation of fibroblasts in the alveolar spaces and interstitium, as well as hyperplasia of type II lung cells, causing the alveolar walls to thicken. Mononuclear inflammatory cells, especially macrophages and lymphocytes, may appear.<sup>40,41</sup> This would account for late radiological findings such as progression of areas of lung consolidation towards a more linear pattern. The end result of the first two phases is deposition of mature collagen, leading to progression towards chronic interstitial fibrosis. However, in patients who follow a favourable course, most fibroblast proliferation resolves with no functionally significant residual fibrosis<sup>42,43</sup> (Fig. 5).

Other histological findings are the appearance of infarctions of the lung parenchyma, alveolar haemorrhage and

fibrin thrombi.<sup>44</sup> Pulmonary infarctions (25% of patients) and alveolar haemorrhage have been reported in patients with a clinical course of more than 10 days. Fibrin thrombi, which are a common finding in diffuse alveolar damage, characteristically affect small-calibre arteries in both early and late stages. It is clear that patients with COVID-19 are in a prothrombotic state, which might be explained by the presence of SIRS, since increased levels of IL-6 and TNF, as well as activation of platelets and damage to endothelial cells, trigger the extrinsic coagulation pathway through tissue factor and the intrinsic coagulation pathway through clotting factors. Thrombin converts fibrinogen to fibrin, which is present in thrombi in small-calibre and distal vessels. As these may interfere with the functioning of various organs, systemic anticoagulation is recommended in patients with COVID-19. It must not be forgotten that the infection itself or sepsis may cause the patient to become dehydrated; this, coupled with other prothrombotic risk factors such as obesity and bed confinement, could account for the relatively common development of pulmonary embolism.<sup>45,46</sup>

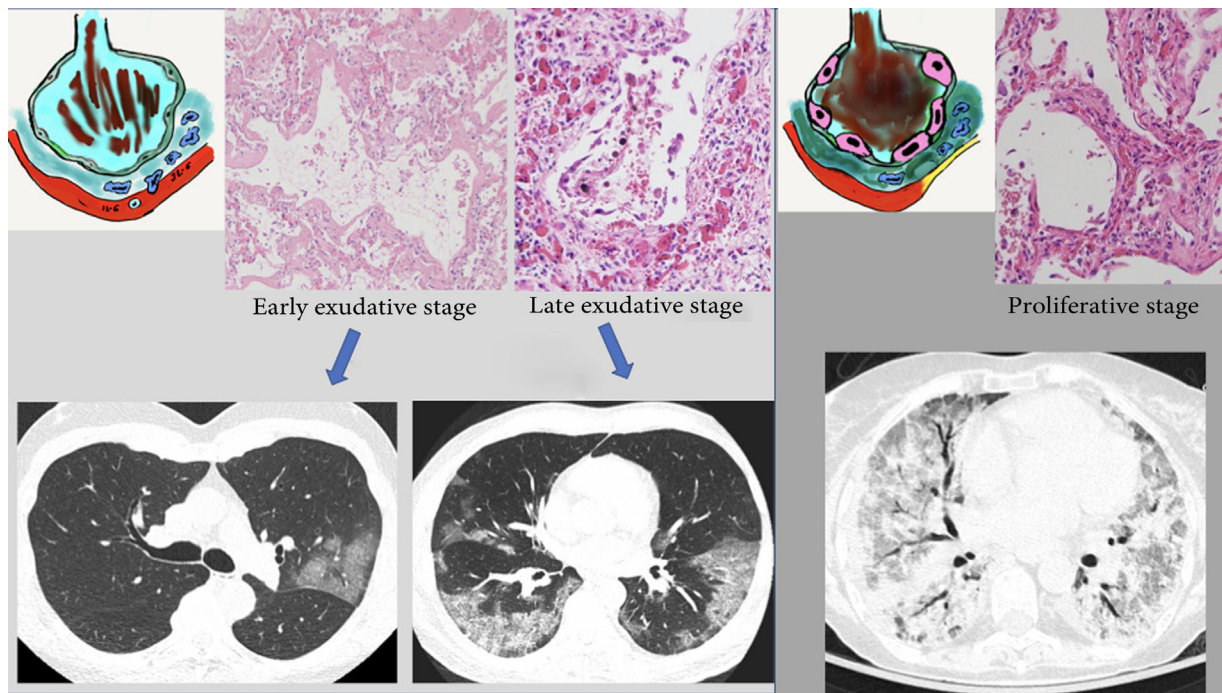


**Figure 5** Proposed radiopathological correlation of the different stages of acute respiratory distress syndrome in COVID-19. A) Exudative or early phase, featuring alveolar oedema with haemorrhage and hyaline membranes. Pro-inflammatory substances (IL-6) with activation of cells (macrophages) causing endothelial damage with vascular ingurgitation. B) Later phase with progression of abnormalities (areas of consolidation). C) Proliferative phase, with large numbers of alveolar hyaline membranes and hypertrophy of type II lung cells. Increase in collagen leading to formation of interstitial fibrosis. Formation of fibrin thrombi (microvascular thrombosis). See text.

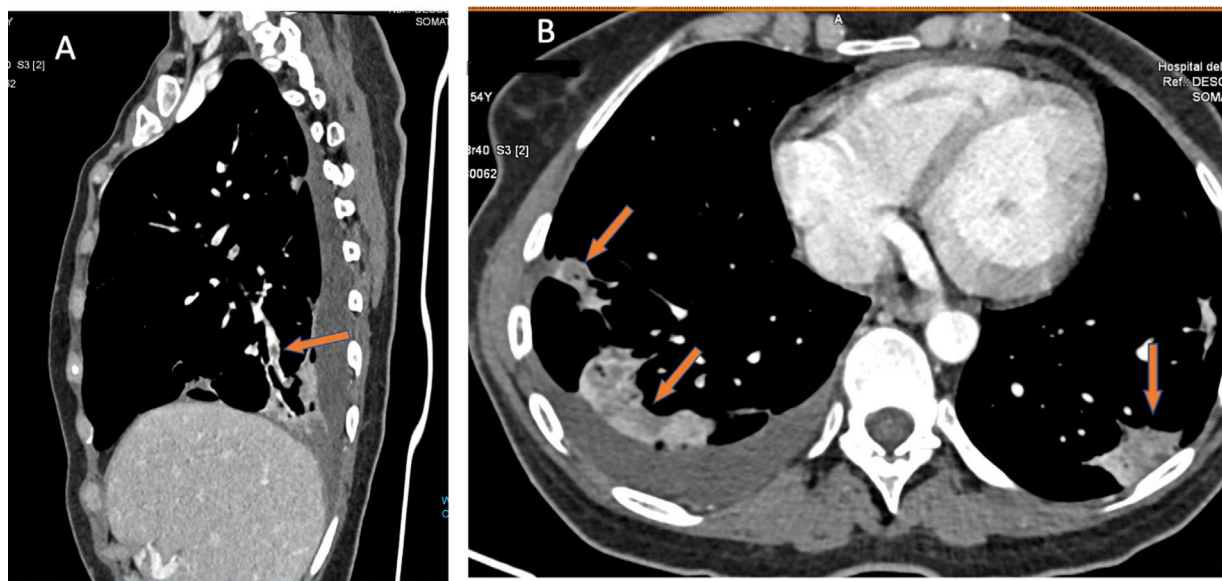


**Figure 6** A patient with COVID-19 and pulmonary thromboembolism. D-dimer 12,556 ng/mL. CT with intravenous contrast. A) This shows filling defects in distal (segmental) pulmonary arteries. B) Strikingly, the axial image shows zones of lower density in the areas of lung consolidation, suggesting zones of infarction. This sign, when detected, should alert the clinician to the possibility of pulmonary thromboembolism and prompt reassessment of distal and small vessels for its presence.

Curiously, on CT scans with evidence of thromboembolic disease, thrombi are usually small, segmental or subsegmental (Fig. 6). This begged the question of whether elevation of D-dimer is due to arterial thrombi so small that they

are invisible on CT given its limited spatial resolution.<sup>47</sup> To answer this question, patients with COVID-19 and elevation of D-dimer were studied. These patients underwent a dual-energy CT scan with contrast. Patients with pulmonary

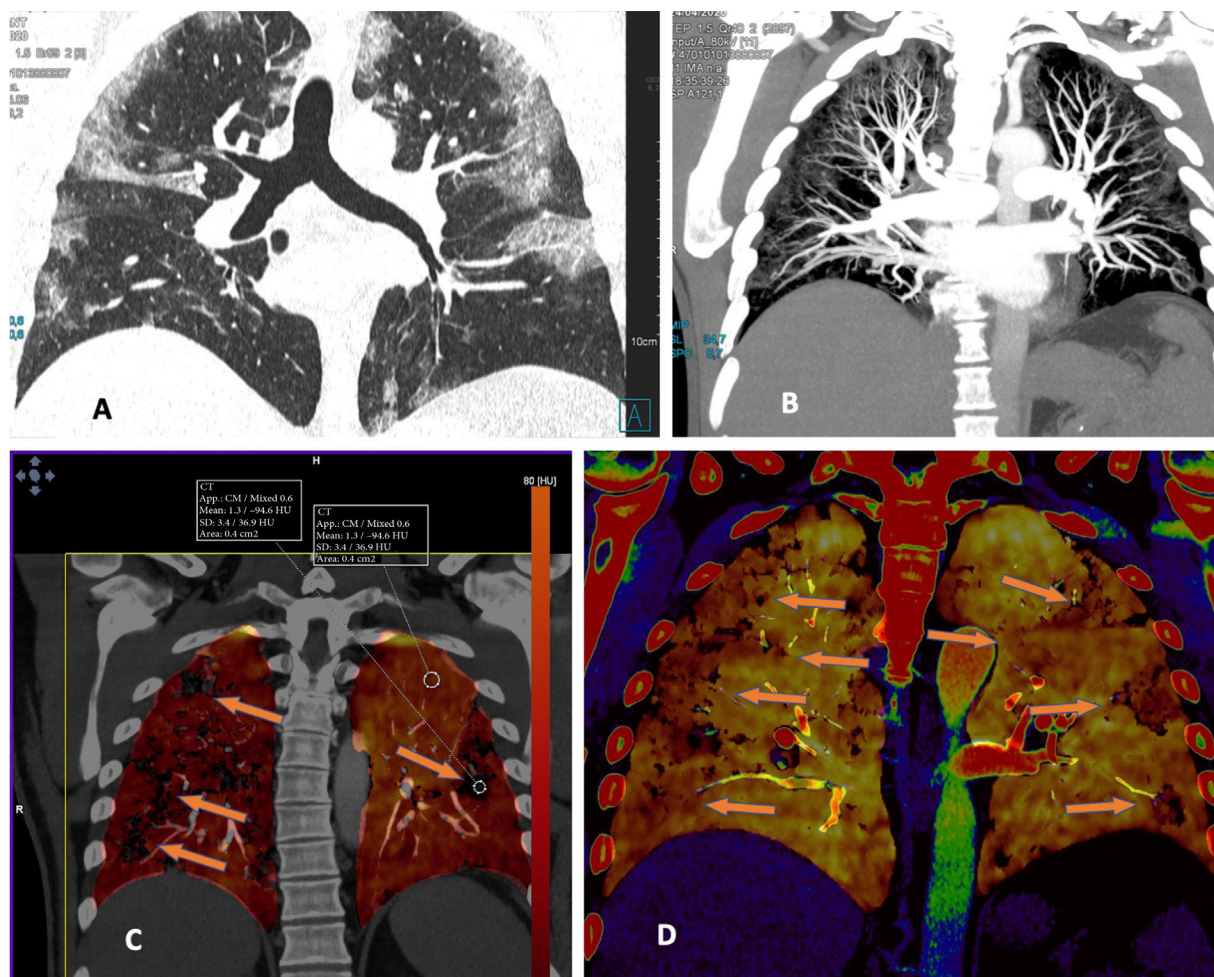


**Figure 7** A woman (healthcare worker) with suspected infection. Positive PCR. Normal chest X-ray. Treatment was started with hydroxychloroquine and azithromycin. Over the next 4 days she showed persistent fever and gradual worsening with dyspnoea and desaturation. Increase in inflammatory markers (IL-6). Elevation of D-dimer from 322 to more than 4000 ng/mL. A) CT, lung window showing extensive bilateral peripheral lesions. B) CT angiography (dual-energy) showing no evidence of pulmonary thromboembolism. Maximum intensity projection (MIP) reconstruction enabling visualisation of distal vessels, including inside areas of lung consolidation. C) PBV imaging (Lung Analysis software program; Siemens Healthineers) showing patchy areas of perfusion defects essentially corresponding to areas of consolidation that exhibit lower contrast uptake (uptake of 1.3 HU) compared to areas of healthy lung (uptake of 63.4 HU). D) Coronal reconstruction with narrower density thresholds, showing lower uptake by peripheral lung areas (hypoperfusion), more pronounced on the right side (see text).

thromboembolism (PTE) showed characteristic perfusion defects associated with areas of lung consolidation that exhibited well-delimited areas of low attenuation in vascular regions without any appreciable arterial thrombus. This finding could be explained by vascular obstruction in small and distal vessels not visible on CT (Fig. 6).

By contrast, patients who did not show PTE and who had extensive disease with multiple lung lesions exhibited patchy areas with lower uptake on pulmonary blood volume (PBV) imaging (a lung perfusion map obtained with dual-energy CT). With the positioning of a region of interest (ROI) in these areas, contrast uptake was found to be lower in them than in healthy lung areas. Construction of colour maps with narrower density thresholds showed areas of pulmonary hypoperfusion (Fig. 7).<sup>48</sup> However, in cases of more minor lesions and milder disease, no perfusion defects were seen (Fig. 8A), and low-energy single-energy (40 KeV)

imaging and reconstructions enabled the patency of more distal vessels to be examined. In addition, ground-glass lesions and, in particular, areas of consolidation could take up contrast; this would support the notion of an inflammatory origin when disease is less extensive and probably also in early stages (Fig. 9). Similarly, nuclear medicine studies conducted using fluorodeoxyglucose (FDG) (<sup>18</sup>F) positron emission tomography/computed tomography (PET/CT) also showed increased metabolic activity in lung lesions, thus confirming the inflammatory component as the most likely cause of lung involvement (Fig. 10).<sup>49</sup> There is no clear explanation for these findings, just as there is no clear explanation for many signs of this disease. However, it could be hypothesised that viral infection of the lungs in early stages has an inflammatory component; in fact, in many cases its radiological behaviour resembles that of cryptogenic organising pneumonia.<sup>36,50</sup> This would explain why the

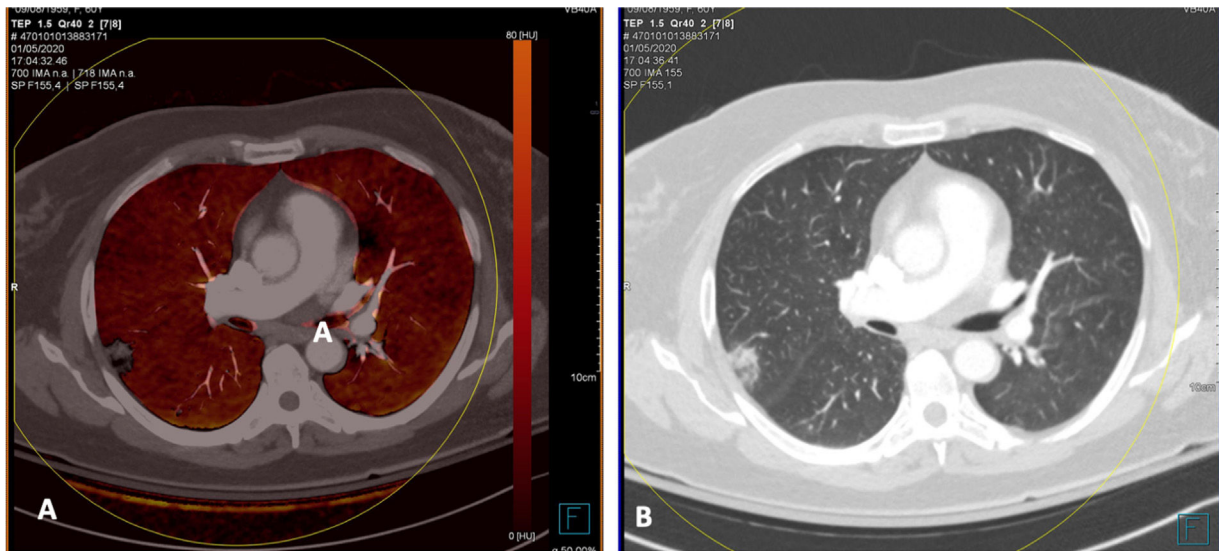


**Figure 8** Patient with COVID-19 who had several pulmonary lesions with high attenuation. Dual-energy CT. CT angiography (dual-energy) showing no evidence of pulmonary thromboembolism (PTE). A) PBV imaging exhibiting no perfusion defects characteristic of PTE and showing homogeneous perfusion of the lung parenchyma. B) Lung window showing one of the lung lesions with the reversed halo sign.

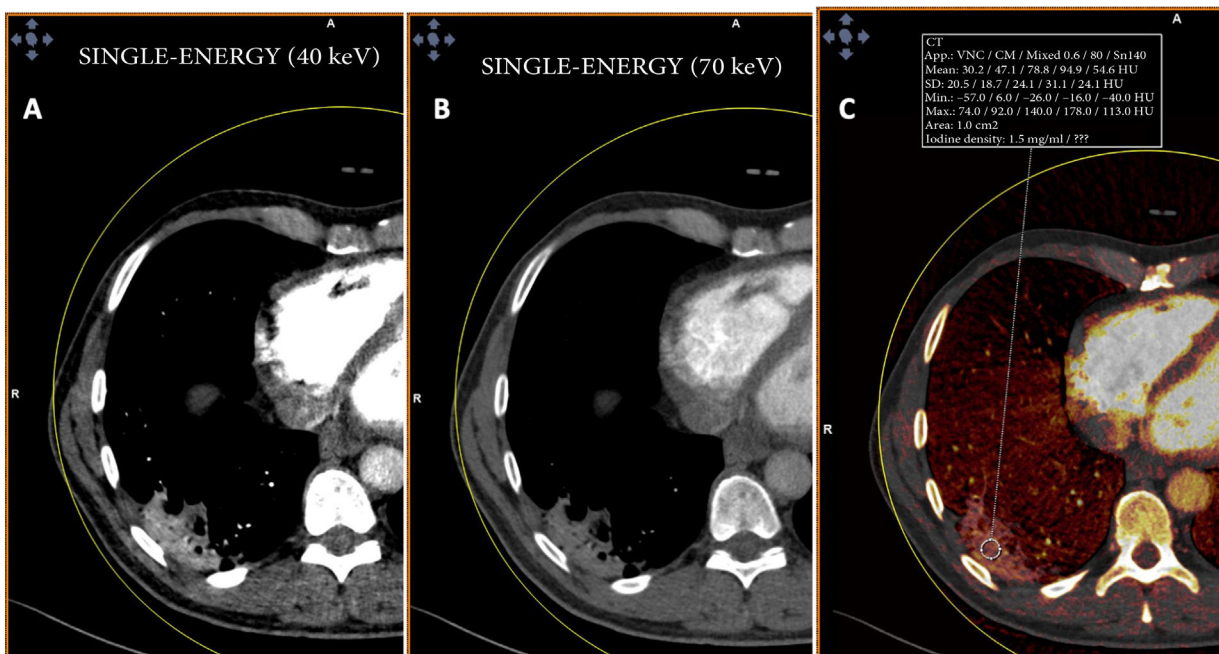


**Figure 9** A patient with COVID-19. Dual-energy CT. A and B) Single-energy imaging showing right posterior and basal consolidation uptake, more obvious on low-energy single-energy imaging (40 KeV). C) Image from iodine map showing lesion uptake with an increase in density of 47 HU.

lesions take up contrast on imaging studies and resolve with anti-inflammatory treatment.

If the disease progresses, the alveolar damage increases; as a result, non-ventilated areas increase and the ventilation/perfusion (V/Q) ratio is altered. That is to say, poorly ventilated lung areas exhibit an arterial vasoconstriction reflex, called the von Euler-Liljestrand mechanism, essentially in the alveolar capillaries, accounting for the zones of pulmonary hypoperfusion in areas with a ground-glass

appearance and consolidation, as well as in adjacent areas. This would amount to compromised ventilation-perfusion in the form of a shunt or short circuit, and would explain the presence of blood gas abnormalities with a decreased PO<sub>2</sub> and an increased alveolar–arterial oxygen gradient. Patients hyperventilate in an effort to increase haemoglobin oxygen saturation; however, in intact lung areas, haemoglobin is saturated (an effect of the oxygen–haemoglobin dissociation curve), yet enables CO<sub>2</sub> elimination, given that the

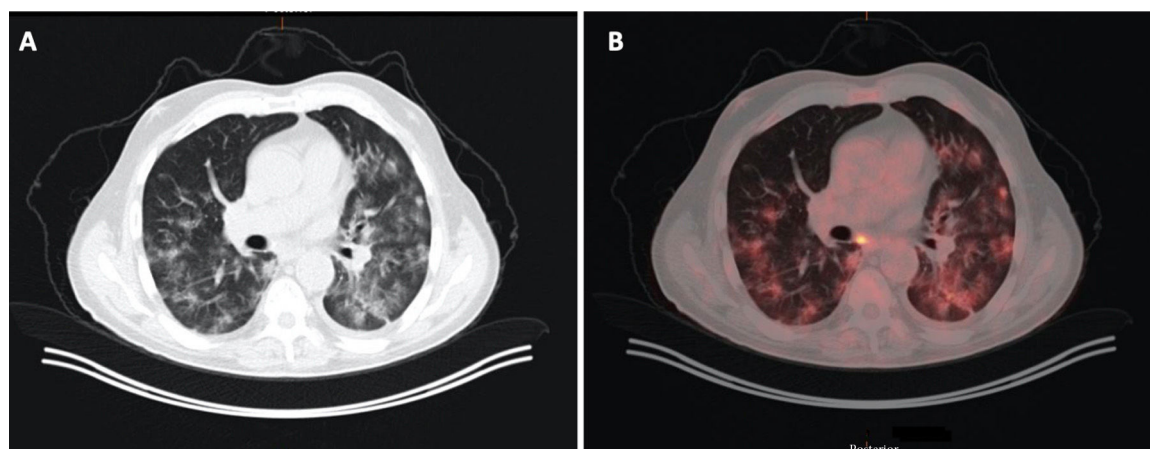


**Figure 10** A 71-year-old man with a history of colon carcinoma, in whom monitoring revealed an indeterminate pulmonary nodule. A) Image from CT with lung window. B) Image from a PET/CT scan showing increased areas of bilateral density characteristic of COVID-19, which exhibit metabolic uptake.

diffusibility of CO<sub>2</sub> is 20 times that of oxygen. This mechanism would shed light on how patients show hypoxaemia with normocapnia or hypocapnia. Administration of 100% oxygen may improve this situation by recruiting some of the altered alveoli.<sup>51</sup>

In conclusion, the SARS-2 virus, a member of the coronavirus family, infects alveolar cells through a binding affinity between ACE2 receptors and the virus's S protein; this binding affinity enables the virus to gain entry into the cell through a mechanism of endocytosis and replicate therein. This mechanism activates innate or cellular immunity as an initial immune response and triggers cytokine production. A poorly regulated response leads to SIRS or cytokine storm, causing cell damage. In the lung, alveolar damage is incurred as part of the inflammatory response, offering an explanation for radiological abnormalities with ground-glass patterns and areas of condensation. A more severe disease course leads to greater alveolar damage and causes a pattern of end-stage ARDS in many patients. Alveolar damage leads to V/Q alteration in the form of a shunt, prompting a vasoconstriction reflex in the lung capillaries, which would explain the areas of pulmonary hypoperfusion seen in perfusion models from dual-energy CT scans, as well as the blood gas abnormalities observed in these patients.

## Authorship

- 1 Responsible for study integrity: GCFP.
- 2 Study concept: GCFP, MOM, MVC, AFL, PFR.
- 3 Study design: GCFP, PFR, MDB, ABL, MCC.
- 4 Data collection: GCFP, MOM, MBD, PFR, JMOC, MCC.
- 5 Data analysis and interpretation: MOM, PFR, MVC, GCFP, MDB, AFL, MCC.
- 6 Statistical processing: N/A.
- 7 Literature search: MOM, MVC, GCFP, MDB, JMOC, AFL, PFR.
- 8 Drafting of the paper: GCFP, MVC, MOM, MCC, AFL, PFR.
- 9 Critical review of the manuscript with intellectually significant contributions: MVC, MOM, MCC, AFL, PFR, MCC, PFR.

- 10 Approval of the final version: GCFP, MOM, PFR, MVC, MCC, MDB, AFL, JMOC.

## Conflicts of interest

The authors declare that they have no conflicts of interest.

## Acknowledgements

We would like to extend our special thanks to Lucía Fernández for her support and for designing the drawings.

## References

1. Chinese doctor, silenced after warning of outbreak, dies from coronavirus. <https://www.nytimes.com/2020/02/06/world/asia/chinese-doctor-Li-Wenliang-coronavirus.html>. New York Times. Published on Feb. 6, 2020.
2. Rolling updates on coronavirus disease (COVID-19). <https://www.who.int/emergencies/diseases/novel-coronavirus-2019/events-as-they-happen>. Updated 29 June 2020. (Accessed 09 July 2020).
3. Kakodkar P, Kaka N, Baig MN. A comprehensive literature review on the clinical presentation, and management of the pandemic coronavirus disease 2019 (COVID-19). *Cureus*. 2020;6:e7560.
4. Morty RE, Ziebuhr J. Call for papers: the pathophysiology of COVID-19 and SARS-CoV-2 infection. *Am J Physiol Lung Cell Mol Physiol*. 2020;318:L1016–19.
5. Rabaan AA, Al-Ahmed SH, Haque S, Sah R, Tiwari R, Singh Y, et al. SARS-CoV-2, SARS-CoV, and MERS-CoV: a comparative overview. *Infez Med*. 2020;28:174–84.
6. Ciotti M, Angeletti S, Minieri M, Giovannetti M, Benvenuto D, Pascarella S, et al. COVID-19 outbreak: an overview. *Chemotherapy*. 2019;64:215–23.
7. Chen L, Liu W, Zhang Q, Xu K, Ye G, Wu W, et al. RNA based mNGS approach identifies a novel human coronavirus from two individual pneumonia cases in 2019 Wuhan outbreak. *Emerg Microbes Infect*. 2020;9:313–9.
8. Hasan A, Paray BA, Hussain A. A review on the cleavage priming of the spike protein on coronavirus by angiotensin-converting enzyme-2 and furin. *J Biomol Struct Dyn*. 2020;22:1–9.

9. Reynolds HR, Adhikari S, Pulgarin C. Renin-angiotensin-aldosterone system inhibitors and risk of Covid-19. *N Engl J Med*. 2020;382:2441–8.
10. Chen L, Hao G. The role of angiotensin-converting enzyme 2 in coronaviruses/influenza viruses and cardiovascular disease. *Cardiovasc Res*. 2020;8 [Epub ahead of print].
11. Chen Y, Liu Q, Guo D. Emerging coronaviruses: genome structure, replication, and pathogenesis. *J Med Virol*. 2020;92:418–23.
12. Jin Y, Yang H, Ji W, Chen S, Zhang W, Duan G. Virology, epidemiology, pathogenesis, and control of COVID-19. *Viruses*. 2020;12:372.
13. Chousterman BG, Swirski FK, Weber GF. Cytokine storm and sepsis disease pathogenesis. *Semin Immunopathol*. 2017;39:517–28.
14. Henderson LA, Canna SW, Schulert GS. On the alert for cytokine storm: immunopathology in COVID-19. *Arthritis Rheumatol*. 2020;72:1059–63.
15. Mehta P, McAuley DF, Brown M, Sanchez E, Tattersall RS, Manson JJ, et al. COVID-19: consider cytokine storm syndromes and immunosuppression. *Lancet*. 2020;395:1033–4.
16. Chau Vq, Oliveros E, Mahmood K, Singhvi A, Lala A, Moss N, et al. The imperfect cytokine storm: severe COVID-19 with ARDS in patient on durable LVAD support. *JACC Case Rep*. 2020;2:1315–20.
17. Zhu J, Ji P, Pang J, Zhong Z, Li H, He C, et al. Clinical characteristics of 3,062 COVID-19 patients: a meta-analysis. *J Med Virol*. 2020;15, <http://dx.doi.org/10.1002/jmv.25884> [Epub ahead of print].
18. Mizumoto K, Kagaya K, Zarebski A, Chowell G. Estimating the asymptomatic proportion of coronavirus disease 2019 (COVID-19) cases on board the Diamond Princess cruise ship, Yokohama, Japan 2020. *Euro Surveill*. 2020;25:2000180, <http://dx.doi.org/10.2807/1560-7917>.
19. Huang C, Wang Y, Li X, Ren L, Zhao J, Hu Y, et al. Clinical features of patients infected with 2019 novel coronavirus in Wuhan, China. *Lancet*. 2020;395:497–506.
20. Holshue ML, DeBolt C, Lindquist S. First case of 2019 novel coronavirus in the United States. *N Engl J Med*. 2020;382:929–36.
21. Chen N, Zhou M, Dong X, Qu J, Gong F, Han Y, et al. Epidemiological and clinical characteristics of 99 cases of 2019 novel coronavirus pneumonia in Wuhan, China: a descriptive study. *Lancet*. 2020;395:507–13.
22. Whittaker E, Bamford A, Kenny J, Kafrou M, Jones CE, Shah P, et al. Clinical characteristics of 58 children with a pediatric inflammatory multisystemic syndrome temporally associated with SARS-CoV-2. *JAMA*. 2020;324:259–69.
23. Landa N, Mendieta-Eckert M, Fonda-Pascual P, Aguirre T. Chilblain-like lesions on feet and hands during the COVID-19 pandemic. *Int J Dermatol*. 2020;24, <http://dx.doi.org/10.1111/ijd.14937> [Epub ahead of print].
24. Suarez-Valle A, Fernandez-Nieto D, Diaz-Guimaraens B, Dominguez-Santas M, Carretero I, Perez-Garcia B. Acroischemia in hospitalized COVID-19 patients. *J Eur Acad Dermatol Venereol*. 2020;7, <http://dx.doi.org/10.1111/jdv.16592> [Epub ahead of print].
25. Connors JM, Levy JH. COVID-19 and its implications for thrombosis and anticoagulation. *Blood*. 2020;(Apr 27), pii: blood.2020060000. doi: <https://doi.org/10.1182/blood.2020060000>. [Epub ahead of print].
26. Gavrilaki E, Brodsky RA. Severe COVID-19 infection and thrombotic microangiopathy: success doesn't come easily. *Br J Haematol*. 2020;189:e227–30.
27. Yang W, Sirajuddin A, Zhang X, Liu G, Teng Z, Zhao S, et al. The role of imaging in 2019 novel coronavirus pneumonia (COVID-19). *Eur Radiol*. 2020;15:1–9.
28. Cheng Z, Lu Y, Cao Q, Quin L, Pan Z, Yan F, et al. Clinical Features and Chest CT Manifestations of Coronavirus Disease 2019 (COVID-19) in a Single-Center Study in Shanghai, China. *AJR Am J Roentgenol*. 2020;14:1–6.
29. Zhang R, Ouyang H, Fu L, Wang S, Han J, Huang K, et al. CT features of SARS-CoV-2 pneumonia according to clinical presentation: a retrospective analysis of 120 consecutive patients from Wuhan city. *Eur Radiol*. 2020;30:4417–26.
30. Salehi S, Abedi A, Balakrishnan S, Gholamrezanezhad A. Coronavirus disease 2019 (COVID-19): a systematic review of imaging findings in 919 patients. *AJR Am J Roentgenol*. 2020;14:1–7.
31. Duan YN, Qin J. Pre- and posttreatment chest CT findings: 2019 novel coronavirus (2019-nCoV) pneumonia. *Radiology*. 2020;295:21.
32. Bernheim A, Mei X, Huang M, Yang Y, Fayas ZA, Zhang N, et al. Chest CT findings in coronavirus disease-19 (COVID-19): relationship to duration of infection. *Radiology*. 2020;20:200463.
33. Song F, Shi N, Shan F, Zhang Z, Shen J, Lu H, et al. Emergency 2019 novel coronavirus (2019-nCoV) pneumonia. *Radiology*. 2020;295:210–7.
34. Cardinal-Fernández P, Corregre E, Villanueva J, Ríos F. Distrés respiratorio agudo: del síndrome a la enfermedad. *Med Intensiva*. 2016;40:169–75.
35. Butt Y, Kurdowska A, Allen TC. Acute lung injury: a clinical and molecular review. *Arch Pathol Lab Med*. 2016;140:345–50.
36. Kligerman SJ, Franks TJ, Galvin JR. From the radiologic pathology archives: organization and fibrosis as a response to lung injury in diffuse alveolar damage, organizing pneumonia, and acute fibrinous and organizing pneumonia. *Radiographics*. 2013;33:1951–75.
37. Bai HX, Hsieh B, Xiong Z, Halsey K, Choi JW, Tran TML, et al. Performance of radiologists in differentiating COVID-19 from viral pneumonia on chest CT. *Radiology*. 2020;296:E46–51.
38. Barton LM, Duval EJ, Stroberg E, Ghosh S, Mukhopadhyay S. COVID-19 Autopsies, Oklahoma, USA. *Am J Clin Pathol*. 2020;153:725–33. *Med Intensiva*. 2016;40:169–175.
39. Franks TJ, Chong PY, Chui P, Galvin JR, Lourens RM, Reid AH, et al. Lung pathology of severe acute respiratory syndrome (SARS): a study of 8 autopsy cases from Singapore. *Hum Pathol*. 2003;34:743–8.
40. Tian S, Xiong Y, Liu H, Niu L, Guo J, Liao M, et al. Pathological study of the 2019 novel coronavirus disease (COVID-19) through postmortem core biopsies. *Mod Pathol*. 2020;33:1007–14.
41. Beigmoammadi MT, Jahanbin B, Safaei M, Amoozadeh L, Khoshavi M, Mehrdash V, et al. Pathological findings of postmortem biopsies from lung, heart and liver of 7 deceased COVID-19 patients. *Int J Surg Pathol*. 2020;19:1066896920935195.
42. Hanley B, Lucas SB, Youd E, Swift B, Osborn M. Autopsy in suspected COVID-19 cases. *J Clin Pathol*. 2020;73:239–42.
43. Carsana L, Sonzogni A, Nasr A, Rossi RS, Pellegrinelli A, Zerbi P, et al. Pulmonary post-mortem findings in a series of COVID-19 cases from northern Italy: a two-center descriptive study. *Lancet Infect Dis*. 2020:201135–40, <http://dx.doi.org/10.1016/S1473-3099:30434-5>.
44. Wichmann D, Sperhake JP, Lütgehetmann M, Steurer S, Edler C, Heinemann A, et al. Autopsy findings and venous thromboembolism in patients with COVID-19. *Ann Intern Med*. 2020;6:M20–2003.
45. Giannis D, Ziogas IA, Gianni P. Coagulation disorders in coronavirus infected patients: COVID-19, SARS-CoV-1, MERS-CoV and lessons from the past. *J Clin Virol*. 2020;127:104362.
46. Lodigiani C, Iapichino G, Carena L. Venous and arterial thromboembolic complications in COVID-19 patients admitted to an academic hospital in Milan. Italy. *Thromb Res*. 2020;23:9–14.
47. Danzi GB, Loffi M, Galeazzi G, Gherbesi E. Acute pulmonary embolism and COVID-19 pneumonia: a random association? *Eur Heart J*. 2020;41:1858.

48. Lang M, Som A, Mendoza DP. Hypoxaemia related to COVID-19: vascular and perfusion abnormalities on dual-energy CT. *Lancet Infect Dis.* 2020;30. S1473-3099(20)30367-4. doi: [https://doi.org/10.1016/S1473-3099\(20\)30367-4](https://doi.org/10.1016/S1473-3099(20)30367-4). [Epub ahead of print].
49. Qin C, Liu F, Yen TC, Lan X. <sup>8</sup>F-FDG PET/CT findings of COVID-19: a series of four highly suspected cases. *Eur J Nucl Med Mol Imaging.* 2020;47:1281–6.
50. Hani C, Trieu NH, Saab I. COVID-19 pneumonia: a review of typical CT findings and differential diagnosis. *Diagn Interv Imaging.* 2020;101:263–8.
51. Sommer N, Strielkov I, Pak O, Weissmann N. Oxygen sensing and signal transduction in hypoxic pulmonary vasoconstriction. *Eur Respir J.* 2016;47:288–303.